

International Journal of Modern Physics E  
 © World Scientific Publishing Company

## MOMENTUM DISTRIBUTIONS FROM THREE-BODY DECAYING ${}^9\text{Be}$ AND ${}^9\text{B}$ RESONANCES

R. ÁLVAREZ-RODRÍGUEZ

*Grupo de Física Nuclear, Departamento de Física Atómica, Molecular y Nuclear  
 Universidad Complutense de Madrid, E-28040 Madrid, Spain,  
 raquel.alvarez@fis.ucm.es*

A.S. JENSEN, D.V. FEDOROV

*Department of Physics and Astronomy, University of Aarhus, DK-8000 Aarhus C, Denmark*

E. GARRIDO

*Instituto de Estructura de la Materia, CSIC, Serrano 123, E-28006 Madrid, Spain*

Received (received date)

Revised (revised date)

The complex-rotated hyperspherical adiabatic method is used to study the decay of low-lying  ${}^9\text{Be}$  and  ${}^9\text{B}$  resonances into  $\alpha$ ,  $\alpha$  and  $n$  or  $p$ . We consider six low-lying resonances of  ${}^9\text{Be}$  ( $1/2^\pm$ ,  $3/2^\pm$  and  $5/2^\pm$ ) and one resonance of  ${}^9\text{B}$  ( $5/2^-$ ) to compare with. The properties of the resonances at large distances are decisive for the momentum distributions of the three decaying fragments. Systematic detailed energy correlations of Dalitz plots are presented.

### 1. Introduction

The structure of the  ${}^9\text{Be}$  nucleus has been considered as a prototype of cluster structure in nuclei. It has been described theoretically by many different cluster models and several experiments have been performed in order to understand its structure and decay mechanisms. Much effort has been devoted to the  $5/2^-$  state due to its astrophysical importance in the formation of  ${}^9\text{Be}$ ,  ${}^{12}\text{C}$  and heavier elements in stellar nucleosynthesis<sup>1,2,3</sup>.  ${}^9\text{Be}$  and  ${}^9\text{B}$  are mirror nuclei that decay into  $\alpha\alpha n$  and  $\alpha\alpha p$  respectively. Therefore their structures are expected to be very similar. We present here the results of two-dimensional energy correlations after the three-body decay of several  ${}^9\text{Be}$  resonances. Moreover the same kind of results for the  $5/2^-$ -resonance of  ${}^9\text{B}$  are shown in order to show the similarities.

### 2. Theoretical Description Of Three-Body Resonances

We employ here the complex-scaled hyperspherical adiabatic expansion method to solve the Faddeev equations which describe our three-body system<sup>4</sup>. The angular

2 *R. Álvarez-Rodríguez, A.S. Jensen, D.V. Fedorov and E. Garrido*

part of the Hamiltonian is first solved keeping fixed the value of the hyperradius  $\rho$ . Its eigenvalues serve as effective potentials while the eigenfunctions,  $\Phi_{nJM}$  are used as a basis to expand the total wave-function  $\Psi^{JM} = \frac{1}{\rho^{5/2}} \sum_n f_n(\rho) \Phi_{nJM}(\rho, \Omega)$ . The  $\rho$ -dependent expansion coefficients,  $f_n(\rho)$ , are the hyperradial wave functions obtained from the coupled set of hyperradial equations<sup>4</sup>.

We consider a two-body interaction able to reproduce the low-energy scattering properties of the two different pairs of particles in our three-body system. Ali-Bodmer  $\alpha-\alpha$  potential<sup>5</sup> and Coulomb potential between  $\alpha$ -particles are considered. The  $\alpha$ -nucleon interaction is taken from Cobis et al<sup>6</sup>. The  ${}^9\text{Be}$ - and  ${}^9\text{B}$ -resonances are of three-body character at large-distances, where they decay into two  $\alpha$ -particles and one neutron or proton, but this is not necessarily the case at short-distances.<sup>7</sup> We use the three-body model at all distances because the decay properties only require the proper description of the emerging three particles. A three-body short-range potential of the form  $V_{3b} = S \exp(-\rho^2/b^2)$  is included to adjust the corresponding small-distance part of the effective potential. The correct resonance energies, which are all-decisive for decay details as evident in the probability for tunneling through a barrier, are then correctly reproduced.

The eigenvalues of the angular Hamiltonian for fixed hyperradius, serve as adiabatic potentials<sup>8</sup>. Each of them correspond to a specific combination of quantum numbers, i.e., partial-wave momenta between two particles in each Jacobi system. Usually few angular eigenvalues are needed for achieving convergence. At small distances the potentials have wells that support the bound states and resonances.

### 3. Energy Distributions

The energy distribution is the probability for finding a given particle at a given energy. It can be measured experimentally and is the only information that allows us to study the decay path. From the theoretical point of view, this information is contained in the large-distance part of the wave function, which must therefore be computed accurately. The Zeldovic regularized Fourier transform of the wave function gives the energy distributions<sup>9</sup>. The resonance wave functions change sometimes substantially from small to large distances. This dynamic evolution allows a better understanding of the decays details<sup>2</sup>.

The decay mechanisms depend on the resonance properties and can be either sequential or direct or a mixture. In our case, all of the resonances can decay sequentially via  ${}^8\text{Be}(0^+)$ , i.e. it is allowed by angular momentum conservation. One of the adiabatic components is related to the  ${}^8\text{Be}+n$  structure and approaches the complex energy of the  ${}^8\text{Be}(0^+)$  resonance. This component will give the sequential contribution<sup>8</sup>.

#### 3.1. ${}^9\text{Be}$

Fig. 1 corresponds to the two-dimensional energy correlations (or Dalitz plots) of the three fragments of  ${}^9\text{Be}$  after the decay. The two possibilities,  $\alpha-n$  and  $\alpha-\alpha$ ,

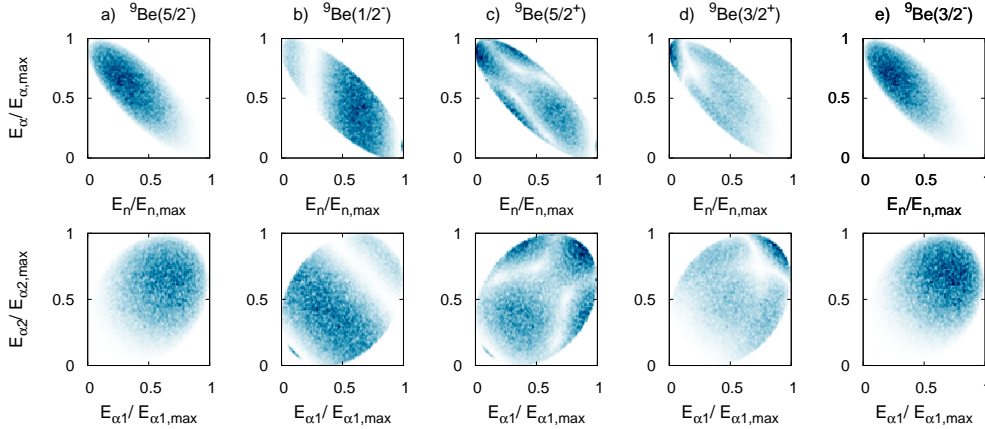


Fig. 1. Dalitz plots for a) the  $5/2^-$ -resonance of  ${}^9\text{Be}$  at 2.43 MeV of excitation energy, b) the  $1/2^-$ -resonance of  ${}^9\text{Be}$  at 2.82 MeV, c) the  $5/2^+$ -resonance of  ${}^9\text{Be}$  at 3.03 MeV, d) the  $3/2^+$ -resonance of  ${}^9\text{Be}$  at 4.69 MeV, e) the  $3/2^-$ -resonance of  ${}^9\text{Be}$  at 5.59 MeV. The upper panels show on the X-axis the neutron energy divided by the maximum possible, and on the Y-axis the  $\alpha$  energy divided by the maximum possible. The lower panels show on X and Y the energy of the two  $\alpha$ -particles divided by the maximum. The sequential decay via  ${}^8\text{Be}(0^+)$  has been removed.

are shown and the  $J^\pi$  of each state is labeled in the figure. The energies are given in units of their maximum values for each case, i.e.  $5/9E_{res}$  for the  $\alpha$ -particles and  $8/9E_{res}$  for the neutrons. In all the cases we have removed the sequential decay via  ${}^8\text{Be}(0^+)$ . It is important to remark that the results are directly comparable to measured distributions.

The first thing that we observe in fig. 1 is that all the plots are symmetric between  $\alpha$ 's energies. This symmetry is necessary since the  $\alpha$ 's are identical particles. The graphs corresponding to  $\frac{5}{2}^-$  and  $\frac{3}{2}^-$ , are very similar to each other. First, we do not observe zeroes in the Dalitz plots.<sup>10</sup> This means that angular momentum conservation does not forbid any energy combination. Second, we see that the density increases towards higher  $\alpha$  energies. This is due to the Coulomb repulsion, which enlarges the charged particles energies while reduces that of the neutron. The other two cases show more structure and have zero probability points or curves.

### 3.2. ${}^9\text{Be}$ vs ${}^9\text{B}$

In our description the only difference between  ${}^9\text{Be}$  and  ${}^9\text{B}$  is the existing Coulomb interaction between the  $\alpha$ -particle and the proton in  ${}^9\text{B}$ . The structure of the resonances in both nuclei are expected to be very similar. Fig. 2 shows the comparison between the Dalitz plots corresponding to the  $5/2^-$ -resonance of  ${}^9\text{Be}$  and  ${}^9\text{B}$ . The patterns are, in fact, almost indistinguishable.

4 *R. Álvarez-Rodríguez, A.S. Jensen, D.V. Fedorov and E. Garrido*

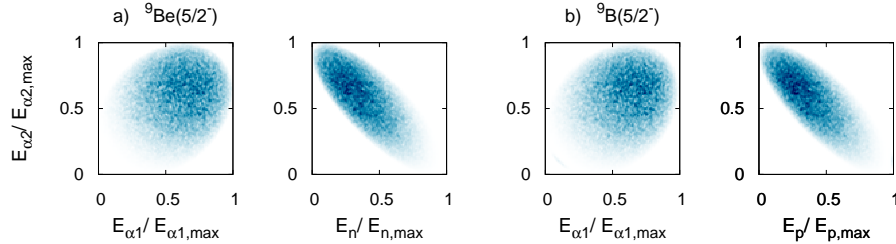


Fig. 2. Dalitz plots for a) the  $5/2^-$ -resonance of  ${}^9\text{Be}$  at 2.43 MeV of excitation energy, b) the  $5/2^-$ -resonance of  ${}^9\text{B}$  at 2.34 MeV. The sequential decay via  ${}^8\text{Be}(0^+)$  has been removed.

#### 4. Summary And Conclusions

We have described  ${}^9\text{Be}$  and  ${}^9\text{B}$  resonances as three clusters by means of the complex-scaled hyperspherical adiabatic expansion method, including short-range and Coulomb interactions. The two-dimensional energy correlations of the decaying fragments are shown for the low-lying resonances of  ${}^9\text{Be}$ . We compare one of them ( $5/2^-$ ) to the corresponding one in  ${}^9\text{B}$  and find, as we expected, an almost identical distribution. Our distributions are open to experimental tests.

#### Acknowledgements

This work was partly supported by funds provided by DGI of MEC (Spain) under the contracts FIS2008-01301 and FPA2007-62216. R.A.R. acknowledges support from Ministerio de Ciencia e Innovación (Spain) under the “Juan de la Cierva” program.

#### References

1. P. Papka, et al. *Phys. Rev. C* **75** (2007) 045803.
2. R. Álvarez-Rodríguez, H.O.U. Fynbo, A.S. Jensen, and E. Garrido, *Phys. Rev. Lett.* **100** (2008) 192501.
3. O. Burda, P. von Neumann-Cosel, A. Richter, C. Forssén, and B. A. Brown, *Phys. Rev. C* **82** (2010) 015808.
4. E. Nielsen, D.V. Fedorov, A.S. Jensen, and E. Garrido, *Phys. Rep.* **347** (2001) 373.
5. S. Ali, and A.R. Bodmer, *Nucl. Phys.* **80** (1966) 99.
6. A. Cobis, D.V. Fedorov, and A.S. Jensen, *Phys. Rev. Lett.* **79** (1997) 2411.
7. E. Garrido, D.V. Fedorov, and A.S. Jensen, *Phys. Lett. B* **684** (2010) 132.
8. R. Álvarez-Rodríguez, A.S. Jensen, E. Garrido and D.V. Fedorov, *Phys. Rev. C* **82** (2010) 034001.
9. D.V. Fedorov, H.O.U. Fynbo, E. Garrido, and A.S. Jensen, *Few-Body Syst.* **34** (2004) 33.
10. H. O. U. Fynbo, R. Álvarez-Rodríguez, A. S. Jensen, O. S. Kirsebom, D. V. Fedorov and E. Garrido, *Phys. Rev. C* **79** (2009) 054009.